

Eco-Friendly Cooking Solutions: Design and Evaluation of Stoves and Briquettes Made from Coal Fines and Sawdust

Musa Alhassan¹, Mohammed Modu Aji^{1,*}, Silas Kiman¹, Abdulhalim Musa Abubakar², Muhammad Abdulrazak³

¹Department of Chemical Engineering, Faculty of Engineering, University of Maiduguri, P.M.B 1069, Maiduguri, Borno State, Nigeria

²Department of Chemical Engineering, Faculty of Engineering, Modibbo Adama University, P.M.B 2076, Yola, Adamawa State, Nigeria

³Department of Agricultural Technology, Federal College of Horticulture Dadin Kowa, Gombe State, Nigeria

*Corresponding author E-mail: moduajim@unimaid.edu.ng

Received: 20 July 2024. Accepted: 27 July 2024. Published: 31 July 2024.

Abstract

Reliance on traditional biomass and fossil fuels for cooking in developing regions poses significant environmental and health challenges. This study addresses the urgent need for sustainable and efficient cooking solutions by developing a novel cooking stove and briquettes using coal fines (CFN) and sawdust (SDT) blends. The primary objective is to enhance fuel efficiency and reduce emissions, thereby providing a cleaner and more affordable cooking alternative. To achieve this, CFN and SDT were blended in varying ratios to produce briquettes, which were then subjected to a series of physical and chemical characterizations, including proximate and ultimate analysis, calorific value (CV) determination, feedstock morphology scrutiny, elemental composition analysis, functional group determination and compressive strength tests. The developed briquettes were used in a specially designed cooking stove, and the performance was evaluated based on combustion efficiency, emission levels, and thermal output. The results indicate that the optimal blend of CFN and SDT significantly improves the CV and combustion efficiency of the briquettes, while reducing harmful emissions such as carbon monoxide and particulate matter. The optimized cooking stove demonstrated superior thermal efficiency and faster cooking times compared to traditional stoves, highlighting the potential for significant fuel savings and environmental benefits. This study has far-reaching implication as it is capable of addressing deforestation, greenhouse gas emissions and poor indoor air quality, thereby contributing to public health and environmental conservation.

Keywords: Coal fines, Sawdust, Briquettes, Cooking stove, Demineralization, Combustion efficiency.

1. Introduction

Waste generation from sawdust (SDT) surpasses 5.2 million metric tons (MMT) in Nigeria, further buttressing the need for its tapping in order to utilize them for solid fuel production for running industries, and for domestic cooking and heating requirements (Elehinafe et al., 2017; Ogunwusi, 2014). SDT generation from log sawmills can be utilized to change the narrative from waste-to-wealth (Mohammed et al., 2014), through the production of briquette whose suitability have been proven in many studies (Elehinafe et al., 2019; Elehinafe et al., 2017; Yang et al., 2021). One of the major problems faced in most parts of the world today and in developing countries (Nigeria inclusive), is the inadequacy of clean and affordable fuel for domestic cooking and other industrial activities; due to the high cost of fossil fuels like kerosene, petrol or liquefied gas for domestic and commercial application (Nwabue et al., 2017). Briquette is a solid energy source that can be produced from domestic, agricultural and industrial sources of biomass waste streams, that is described as sustainable, eco-friendly (eliminate deforestation) and having the potential to reduce the over-dependence on fossil fuel (Akolgo et al., 2021). Most developing nations like Nigeria, largely depend on conventional fuels such as fuelwood (firewood and charcoal), for heating and cooking applications (Ajiboye et al., 2016; Brenda et al., 2017). Kerosene and cooking gas are known to release greenhouse gas emissions (CO_x, SO_x & NO_x), contributing to global warming and a threat to human and animal health (Ajiboye et al., 2016; Nwabue et al., 2017). Over

80% of Nigerians that live in rural and semi-urban areas depend solely on fuelwood for their energy needs while between 37-51% of the total energy demand of the country is accounted for by the fuelwood. Consequently, the need for renewable and viable alternative energy sources due to fast depletion of non-renewable types, fossil fuel shortages, increasing fuel prices, global warming and environmental problems, is desired (Ajiboye et al., 2016; Davies et al., 2013).

Coal fines (CFN) briquette have good hydrophobicity, which influences their physical and combustion properties, making them a competitive solid fuel globally, as confirmed by Massaro et al. (2014). Previously, Manyuchi et al. (2018) produced briquette from CFN and reported briquette with high shatter index, characteristic ease in ignition and efficient calorific values (CV). In their study, Adeleke et al. (2019) reported that CFN are always regarded as waste and low energy realizing feed material when used in industries as fuel – but revealed that when densified as solid briquette fuel, they have high CV and good combustion behavior. In another study, Zhong et al. (2017) noted that the recycling of CFN by processing it to produce coal briquettes, has boundless importance in saving resources that would have been lost, thereby keeping the environment free of pollution and health hazards. Lubwama et al. (2020) revealed that, in order for briquettes to make a substantial dip in charcoal and firewood application in sub-Saharan Africa, mixing of different agricultural residues (including SDT) must be considered in

their totality, simply because of the growing energy demand and increasing population in the region. Bonsu et al. (2020) mentioned that adequate utilization of briquettes would assist in this direction, together with SDT blend proposed by this study. Already, Pontevedra et al. (2019) produced composite briquette blend from coconut shell and madan wood waste, and discovered an end-result with good CV. Brunerová et al. (2018) revealed that briquette production from bamboo fibre and sugar skin as feed material, are highly suitable agro-waste for its manufacture. Elehinafe et al. (2017) and Ogunwusi (2014) relates that one of the woody biomass resource available in huge quantity is SDT, and is generated during the processing of log at sawmills. They also revealed that waste generated in form of SDT amount to over 5.2 MMT in Nigeria. A study by Mohammed et al. (2014) also revealed that in Northeastern Nigeria, only over 1 MMT of organic waste (SDT inclusive) is generated annually. Previously, Onoduku (2014) characterized Maiganga coal sample and discovered its potential as a good source of heat energy for industrial application (e.g., blast furnace operations). Acting on the above merits, the primary objective of this study is to develop an innovative cooking stove and briquettes using blends of CFN and SDT, which is aimed at providing a sustainable and efficient cooking solution. This research seeks to address the environmental and health issues associated with traditional biomass and fossil fuel usage, by creating an alternative that reduces emissions and enhances fuel efficiency. Furthermore, the research will try to optimize the blending ratios of CFN and SDT so as to produce briquettes with improved CV and combustion efficiency. Additionally, the study focuses on designing and evaluating a cooking stove that maximizes the performance of these briquettes, ensuring faster cooking times and safety. In view of that, a series of characterization was conducted.

2. Methods and material

2.1. Materials, Chemicals and Preparatory Steps

Materials used in this work include Maiganga coal from Gombe coal mine in Gombe State, Nigeria. SDT was obtained from sawmill at Tashan Bama, while Gum Arabic was purchased from Gamboru market, both located in Maiduguri, Borno State, Nigeria. It is worthy of note that the SDT was collected in real time. By implication, SDT was collected immediately with a clean pan making it free of unwanted particles (viz., stone, sand or lumps of wood), as it is generated during saw operations. Hydrochloric acid (HCl) and sodium hydroxide (NaOH) of $\geq 99\%$ purity was purchased around Mara-Zaine Area of Maiduguri, Borno State. Distilled water used was produced at the Chemical Engineering Department of the University of Maiduguri, Nigeria. The method adopted in preparing the CFN were those reported by Okoro et al. (2018). SDT preparation was as described by Adeleke et al. (2019, 2021). Gum Arabic binder preparation method was in accordance with Elinge et al. (2019). And lastly, the production of the briquette blends mix was based on Adeleke et al. (2021) description.

Essentially, a locally made mortar and pestle was employed for the preparation of the binder and about 120 μm sieve manufactured by Maharashtra (India), was employed for the screening of the required bulk sample size. Dried Gum Arabic used herein, was purchased at custom market, Maiduguri, Nigeria. Note that an SF-400D electronic weighing balance manufactured by Quincy, was used to measure the desired sample quantity whether CFN, SDT or binders used. Metal sheet, 20 L thinner bucket, anthill/clay, crucible, pH meter, oven, beakers, round bottom flasks and funnels, were all used at different stages of the production and characterization process. Equipment and materials used for the construction of the cooking stove were chisel, hammer, scribe, divider,

hacksaw, steel rule, vice/clamp and bench, snip, metal bucket, welding and drilling machines, mild steel, tape, anthill and clay.

2.2. Coal Sample Feedstock Sourcing

Coal samples were obtained from Garin Maiganga located within the Gombe Formation in Maiganga village, Akko Local Government Area of Gombe state, Nigeria. All samples were initially crushed and pulverized. The coal sample were prepared using both the mechanical and manual methods so as to meet the desired analytical specifications using an array of sample preparation equipment. Crushing of the samples from a top-size of about 500-600 mm, to a suitable size distribution range of 30.5-100 mm, were carried out manually via the use of hammer. A pulverizer was then used to prepare samples from a top size of 6 mm down to a suitable size distribution range of 150-250 μm . An automatic sieve shaker was used for sieving the samples to the desired size distribution required for each test. Similar method was reported by Okoro et al. (2018), which was adopted for this research work.

2.3. Coal Fines Demineralization and Carbonization

Herein, CFN followed 2-step demineralization processes. Initially, 50 g (120 μm) of the CFN was measured in a 500 mL beaker while 2M solution of NaOH was prepared. Subsequently, the mixture was stirred for 2 h at 65°C and at 250 rpm, while immediately repeating the same procedure for HCl. Next, the demineralized CFN were filtered using the Whitman filter paper and then washed with distilled water to achieve a cleaner sample. It was oven-dried at 105°C for 1 h and then kept in a desiccator for carbonization purposes. At this stage, the optimal carbonization temperature adopted for the coal demineralization was 260°C for over 1 h, utilizing an electric furnace. After the process was completed, the carbonized CFN samples were also placed in a desiccator for 1 h and kept ready for densification process. Rahman et al. (2017) reported the same method followed in this research with few modifications made (use of stirrer to aid reaction). Flow of the demineralization and carbonization processes carried out on the CFN and SDT was as shown in Plate 1.

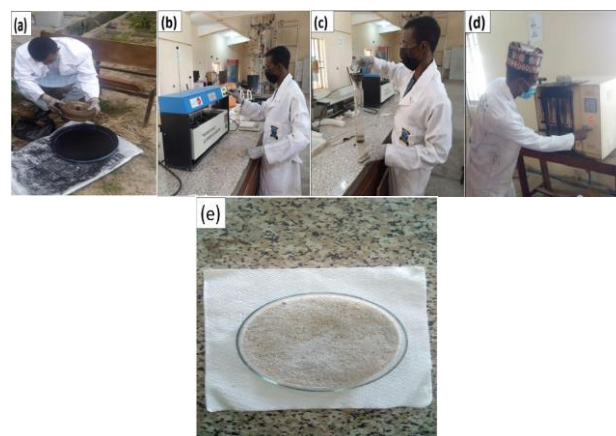


Plate 1: Demineralization and Carbonization stages: (a) Sieving to 120 μm , (b) Raw Coal 2-Step Alkaline and Acid Demineralization, (c) Washing, (d) Carbonization and (e) Pulverized Gum Arabic Densification of the Mix.

2.4. Briquetting Densification Process

The densification process of the briquette blend was based on Adeleke et al. (2021), with a slight modification in the curing days. Each CFN/SDT briquette blend or composite formation using Gum Arabic as binder, is made up of 180 g of the composite materials with 20 g (10%) of Gum Arabic, making it a total of 200 g briquette blend. Using a weighing balance, 180g of the CFN and SDT was measured and thoroughly mixed

in a rubber container and kept aside before mixing with the Gum Arabic binder. About 20 g of the Gum Arabic was weighed and somewhat cold/warm water (50 mL at 30°C) was used to make a slurry paste. Subsequently, the paste was effectively mixed with the composite CFN and SDT earlier measured (180 g) with additional 250 mL of same water, to achieve homogeneity of the mixture. The well mixed blend was then subjected to the mold to hydraulically densify (compact) them at a pressure of 7 MPa using a 3-ton hydraulic press. It is important to mention that this process was perfectly conducted for all the briquette blends keeping in mind their varying but known ratios. All the produced blends were firstly sun-dried immediately after production to allow dryness of the moisture content for only 10 min before oven-drying for 30 min and curing at room temperature for 7 days, before subjecting them to series of characterizations. Five (5) sets of the CFN/SDT feedstock, namely, CFN/SDT (20/80), CFN/SDT (40/60), CFN/SDT (50/50), CFN/SDT (60/40) and CFN/SDT (80/20), was produced with a constant input of the Gum Arabic binder (10%) and 15 s holding time. Plate 2 displays the flow of the briquetting densification processes carried out for the manufacture of the briquette blends.

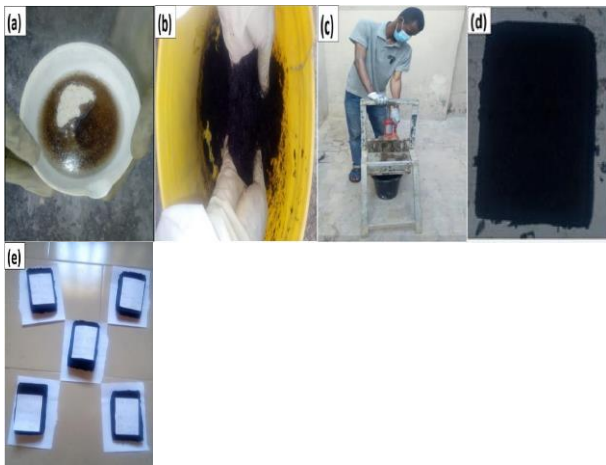


Plate 2: Briquette Production Flow: (a) Binder Slurry, (b) Feedstock Mixing, (c) Densification, (d) Briquette Sample and (e) Five Briquette Blends

2.5. Proximate Analysis

Moisture content (MC) of the coal was calculated from the loss in mass for 1.5 h and 105°C, as specified in ASTM D3173. Volatile matter content (VM) was determined in accordance with the method specified in ISO 562:1998. Ash content (AC) determination was in accordance with the ISO 1171:1997. Lastly, the fixed carbon content (FC) was calculated from the formula used by Akpenpuun et al. (2020) for each of the briquettes developed.

2.6. Briquette Blends Physical Properties

2.6.1. Shatter Index

To measure the shatter index (SI), which represents the measure of shear and impact forces a briquette can withstand during handling, storage and transportation processes, it was dropped on a metal base from a height of 2 m. At this juncture, the mass of the disintegrated briquette was noted. SI was expressed and computed following Equation 1 obtained in Rahaman and Salam (2017).

$$SI = \frac{W_{fn}}{W_{in}} \times 100\% \quad (1)$$

Where W_{fn} = mass of unshattered briquette (g) and W_{in} = initial mass of briquette (g).

2.6.2. Bulk and Relaxed Density

Bulk density (D_{Bulk}) of the briquettes was found based on literature reports (Mandal et al., 2018; Rahaman and Salam, 2017), and calculated using Equation 2. The relaxed density (D_{Rlx}) of the briquettes was based on Bello and Onilude (2020) and Manouchehrinejad et al. (2018), as well as Equation 3.

$$D_{Bulk} = \frac{W_b}{V_b} \quad (2)$$

$$D_{Rlx} = \frac{W_r}{V_r} \quad (3)$$

Where W_b and W_r = weight of the powdered briquette in its dry condition (g) and V_b and V_r = volume of the powdered briquette using a 10 cm³ measuring cylinder.

2.6.3. Hydrophobicity Test

Hydrophobicity (HP) is a measure of percentage of water gained by a briquette when immersed in water. Each briquette was immersed in 150 mm of water column at room temperature for 30 s. The percent of water absorbed by the briquettes (WAB) were recorded and calculated using Equation 4. HP percent was then determined using Equation 5.

$$WAB (\%) = \frac{W_2 - W_1}{W_2} \times 100 \quad (4)$$

$$\text{Hydrophobicity} (\%) = 100 - WAB \quad (5)$$

Where, W_1 = initial mass of briquette (g) and W_2 = mass of wet briquette (g).

2.7. Briquette Blends Combustion Properties

2.7.1. Calorific Value

CV (MJ/kg) of the fuel briquettes were determined using Equation 6 (Sajadi et al., (2021)).

$$CV = -0.8738N \times H^{-1.3101} - 0.1583C \times O^{0.3497} + 0.3856C \times (HO)^{0.1462} + 2.1436 \times \left(\frac{H}{O}\right)^{-0.3846} + 0.1076C \times H^{-0.3846} + NS - 11.2794 \left(\frac{H}{C}\right) \quad (6)$$

Where, N = elemental nitrogen, C = elemental carbon, H = elemental hydrogen, O = elemental oxygen and S = elemental sulphur.

2.7.2. Ignition Test, Burning Time and Rate

Ignition time (IT) was determined based on Ikelle and Ivoms (2018) description, without any modification. The different samples were ignited at the edge of their bases with a Bunsen-burner. The time taken for each briquette to catch fire was recorded as the IT using a stopwatch. On the other hand, the burning time (BT) test was conducted based on Abdullahi et al. (2021) findings. It is the time taken for each briquette sample to burn completely to ashes. Finally, the burning rate (BR), which is the fixed mass ratio of each of the briquette samples to the BT, were also determined based on Equation 7.

$$BR = \frac{\text{Mass of Briquette (g)}}{BT (\text{min})} \quad (7)$$

2.8. Ultimate Analysis

Briquette (powdered) sample passing through a sieve having an aperture of 212 μm was used for this analysis. Ultimate analysis was carried out using the TRUSPEC CHN Elemental determinator. The equipment was supplied with a reference material with known ultimate analysis result. This reference material (Prox-Plus) was used to determine the accuracy of the CHN Elemental determinator before commencing the tests. Precisely 1.0 g of sample was loaded into porous crucibles and subjected to combustion in an oxygen-rich environment. Typical run duration was about 10 min. The system converts the sample catalytically to N, carbon dioxide (CO_2) and water, which are separated with a gas chromatographic column and detected through a sensor. The results were displayed on the computer monitor in terms of percentage C, H and N on an air-dried basis, based on ISO 12902 – CHN instrumental method. Oxygen was calculated by subtracting the cumulative of other elemental compositions on an air-dried basis using Equation 8.

$$O_2(\%) = 100 - (C + H_2 + N_2 + \text{Ash} + MC) \quad (8)$$

Moving on, the elemental H composition was determined using Equation 9 presented by Aliyu et al. (2020).

$$H(\%) = \frac{0.036FC + 0.086(VM - 0.1AC)}{-(0.0035MC^2)(1 - 0.02MC)} \quad (9)$$

Where FC, VM, AC and MC still retain their earlier definitions, determined via proximate analysis.

2.9. SEM, AAS, Characterizations

These characterization methods were similar to those used in previous related studies (Behera & Chakraborty, 2018; Ghorai et al., 2019; Rimmer & Wei, 2018). They include:

2.9.1. SEM Analysis

Mineralogical, morphological and microstructural characterization of the best performing briquette sample, as well as the raw and treated coal samples, were carried out using JEOL-JSM IT 300 LV (Germany) Scanning Electron Microscopy (SEM) analyzer. For each test, microscopic amounts of the samples were sprinkled on the SEM carbon stubs. Next, the samples were sputter coated with platinum using the Quorum Q150R S Sputter coater for 10 min before the SEM/EDX analysis. The analysis was performed at 20 kV and 5 mm working distance to obtain micrographs at magnifications of $\times 1000$. The AZTEC EDX software from Oxford Instruments, UK, was used to analyze the captured SEM images.

2.9.2. AAS Analysis

Filtrates from the demineralized coal that followed 2-step demineralization processes were subjected to Atomic Absorption Spectroscopy (AAS) analyzer before and after washing to examine the extent of demineralization of the coal samples. About 100 ppm was prepared as working solution from the 1000 ppm obtained from manufacturers (Buck Scientific, USA). A simple dilution formula ($C_1V_1 = C_2V_2$) was used to calculate the volume of the stock solution to be diluted to the new desired concentration. To prepare 100 ppm, 10 mL of the standard stock solutions were pipetted and added into 100 mL calibrated flasks. It was finally diluted with deionized water and mixed thoroughly. The other standard working solutions were prepared from the 100 ppm by pipetting out appropriate volume into calibrated flasks, and made up to volume with deionized water. The concentrations of elements in the samples were determined using AAS 210 VGP, Buck Scientific Company, USA). A standard calibration curve was prepared, from which the analytes concentrations were

extrapolated. Concentrations of the element present in the sample were determined by reading their absorbance. Three replicate determinations were carried out on each sample. The element was determined by absorption/concentration mode and the instrument readout was recorded for each solution manually. The same analytical procedure was employed for the determination of element in digested blank solutions and for the spiked samples.

2.9.3. EDXRF Analysis

Ash compositions of the samples were carried out using Energy Dispersive X-ray Fluorescence (EDXRF). The sample was placed in a sample holder contained in the EDXRF equipment and oriented to an angle of 45° . The EDXRF machine was closed and the window of the EDXRF tube was opened 35, via the shutter. The filament voltage was then set progressively to 40 kV and the current to 20 mA. A silicon drift detector was used to detect the secondary X-rays (X-ray detector) and to record the spectrum (acquisition and processing system). Then each element presence was displayed in percentages.

2.9.4. XRF Analysis

X-ray Diffractometer (XRD) analysis of the samples was carried out on the Rigaku XRD, with Cu (K-alpha) as a source of X-rays. The radiations were generated at a tube voltage of 40 kV and tube current of 25 mA. The XRD patterns of the 2 θ versus intensity for an angular range of 2-37 $^\circ$ were obtained. The Joint Committee on Powder Diffraction Standard Mineral Powder Diffraction Files were used for interpreting the diffractogram using the Hanawalt methods of qualitative analysis.

2.9.5. FTIR Analysis

Fourier Transform Infrared Spectroscopy (FTIR) analysis technique detects various characteristic functional groups that are present on the surface of the raw and treated coal samples. When the surface catalyzed adsorbent interacts with infrared light, the chemical bond stretches contracts or bends. As a result, each functional group tends to absorb infrared radiation in a specific wavelength range. The FTIR imaging was carried out using Perkin Elmer RX. The FTIR spectra were collected in the range of 4000-400 cm^{-1} . Potassium bromide (KBr) pellet was first prepared by mixing about 0.01 g of powdered coal sample with about 0.3 g of KBr (Merck; for spectroscopy) in an agate mortar. The mixture was compressed under certain pressure in a special die to form a small disk.

2.10. Stove Design Considerations

Engineering design principles for effective performance such as the stove casing, in this circumstance, was used following Table 1.

Table 1: Stove Design Dimensioning

Material	Dimensions	Values
20 L Thinner Bucket	Height: Volume:	36 cm 20 L
Anthill/clay Insulating Material	Compressive Strength: Thermal Conductivity: Bulk Density:	333.4 N/m ² 0.0032 W/m ² K 9.5 g/cm ³
Mild steel Star Grate	Length: Density:	8 cm 7860 kg/m ³
Firebox/combustion Chamber	Cross Sectional Area: Height:	132.67 m ² 31.5 cm
Pot Placers	Diameter:	29.5, 24 & 14 cm
Stove Handle	Length:	57 cm
Stove Fixed	Diameter:	6 cm

Chimney	Length:	2.5 cm
Air Inlet for Combustion Reaction	Length:	7.5 cm

The stove design was performed using CAD software showing a 2D and 3D pictorial representation of the intended system. Apparently, Figure 1 presents a well labelled schematic of the developed briquette stove in both 2D and 3D form.

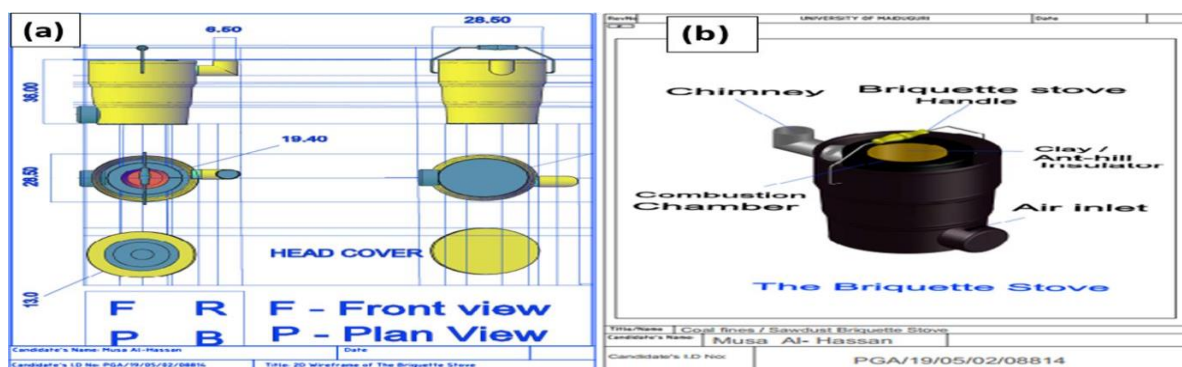


Figure 1: Schematics of the Developed Stove: (a) 2D and 3D of the Stove and the (b) Fully Labelled Diagram

2.10.1. Stove Construction

The stage-wise procedures followed are as follows: dimensioning - marking out - cutting - chiseling and bending – machining - welding – finishing. After procuring the required material for the work, dimensioning of the pot placer with the use of measuring tape was carried out. Combustion chamber insulator mold support including the aluminum metal of the chimney, were all dimensioned. After the dimensioning, they were all marked out using scribe and other marking instrument like permanent marker, so as to ease cutting. The cutting operation was performed using hacksaw on bench held clamps. Gas cutting was performed on the bucket at the chimney position and the air inlet combustion point of the stove. It is important to note that the anthill/clay insulators were molded and cured separately with the appropriate dimensions before inserting and clamping it within the combustion chamber support and the fixed pot placer at the top of the cooking stove with 3 pot placer markings. Tightening clip was cut while some holes were drilled close to the top of the pot placer and the combustion chamber support to enable clipping them together thereby acting as support to the molded anthill and clay insulators within the stove. Drilling and smooth grinding of the 3 removable pot placers was carried out using machine tools and driller. Welding was performed within the cook stove. It is necessary to ascertain its firmness and zero leakage, which could lead to heat loss to the environment. Finally, painting of the cooking stove with chocolate color for beautification, was the finishing touch giving to the constructed stove. The construction was based on Oyejide et al. (2019), with modified chimney material being aluminum. Table 2 presents the cooking stove design specifications.

Table 2: Calculated Stove Design Specification Summary

Stove Parts	Symbol	Design Specifications
Height of the Stove	Hs	36 cm
Outer Diameter	Od	28.50 cm
Stove Cross-Sectional Area	As	637.61 cm ²
Height of Combustion Chamber	Hc	31.5 cm
Combustion Chamber Cross sectional Area	Ac	132.67 cm ²
Removable Chimney Pipe Diameter	Drcp	7.5 cm
Removable Chimney Pipe Length × Breadth	L×B	7.5 cm × 7.5cm
Stove Fixed Chimney	Dsfc	6cm

Diameter		
Stove Fixed Chimney	Lsfc	2.5 cm
Length		
Pot Placers Diameter	Dpp	29.5, 24 & 14 cm
Air Inlet for Combustion	-	7.5 cm
Reaction		
Stove Handle	-	57 cm

2.10.2. Water Boiling Test and Stove Performance Evaluation

Water boiling test (WBT) was carried out to compare the cooking efficiency of the developed briquette blends with the conventional firewood and charcoal. Time taken for 100 g of each briquette blend and same mass for the firewood and charcoal to boil water to 100°C in a stainless-steel pot with the developed cooking stove, was recorded using stop watch and clinical thermometer. Percentage heat utilized (PHU – thermal efficiency) was determined from the WBT data to evaluate the performance of the developed cooking stove using Equation 10 found in Oyejide et al. (2019).

$$PHU = \frac{m_n C_p (T_b - T_o) + m_e L}{m_f H_v} \times 100\% \quad (10)$$

Where, m_n = mass of water in the pot (kg), C_p = specific heat of water (kJ/kg/°C), T_o = starting temperature of the water (°C), T_b = boiling temperature of the water (°C), m_e = mass of water evaporated (kg), L = latent heat of evaporation (kJ/kg), m_f = weight of fuel burnt (kg) and H_v = heating value of the fuel (kJ/kg). Figure 2 shows the schematic diagram of the entire research work.

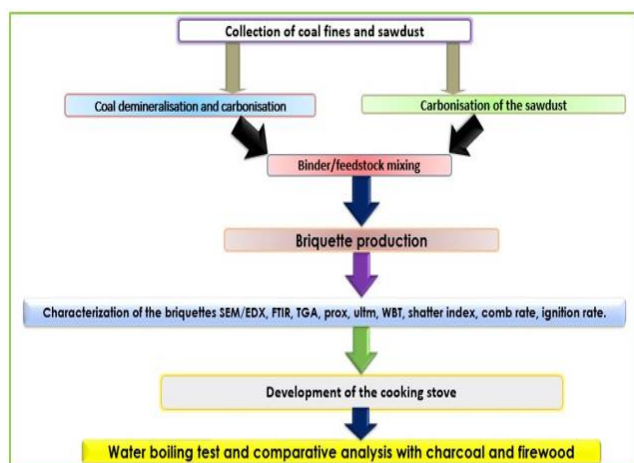


Figure 2: Schematic Diagram of the Entire Research Work

RESULTS AND DISCUSSION

3.1. Developed Stove

The developed briquette stove can be used for daily cooking and heating applications. Pot placers are removable, because of the various diameters of cooking pot, making it easy for the chef to place the right pot with equivalent diameter. As it is, the pot placer and the handle of the stove, makes it stress-free for the user to lift it to any location (cooking/heating point). At the bottom is an air inlet for combustion reaction. This is where air supply gets into the stove and meet the ignited briquette blends that aid combustion. The chimney is removable too and may be removed in the absence of smoke. At the interior is the star-like grate which allows a space for air-supply to the burning briquette, and as well serve as briquette placers. Thus, as they are being consumed, more can be fed or put into the stove for more fuel to be burnt. Finally, in the internal is the molded anthill insulator which prevents heat loss to the environment. Normally, the developed briquette blends releases heat during combustion process. Plate 3 shows the completely developed cooking stove.

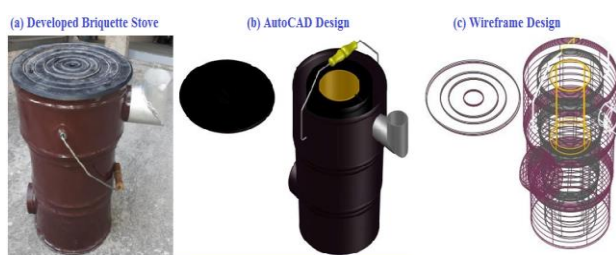


Plate 3: The Cooking Stove Developed

For a family of 5 using a pot of 30 cm diameter, it is suggested that the cross-sectional area of the stove be between 600–700 cm² and height of the combustion chamber be around 30–35 cm. Other measurements such as chimney, grate and stove handle, should be appropriately set to fit the design outlook as described by Oyejide et al. (2019). Mild steel has higher and better properties such as thermal expansion, force, density, tension, elasticity, stiffness, strength and so on. These properties are what influence the choice of metal selection when compared with other types of steel for the pot placers and star grate. The anthill is also favorable considering its physical and thermal properties such as D_{Bulk} , porosity, permeability and thermal conductivity, as described by Khatib et al. (2020) and Okino et al. (2021).

3.2. Briquette Blends Proximate Analysis

MC values of all the briquette blends produced is between 0.53-1.11% which is the standard value set at 7 days of curing (Yank et al., 2016; Mandal et al., 2018; Adeleke et al., 2019), with CFN/SDT (60/40) showing the least at 0.53% as presented in Table 3. This could be due to the demineralization and carbonization pretreatments carried out on both the CFN and the SDT, helping in improving the surface area and ease in interlocking during densification. It is observed that the MC for CFN/SDT (50/50) is the highest at 1.11%, which is attributed to water molecules possibly remaining in the inter-particle opening after densification. This reason is in harmony with Yank et al. (2016) who reported the same scenario from their produced briquette.

Table 3: Proximate Analysis Data

S/No.	Briquette Name Tag	MC (%)	AC (%)	VM (%)	FC (%)
1.	CFN/SDT (20/80)	0.58	13.33	20	66.09
2.	CFN/SDT (40/60)	1.02	16.67	20	62.31
3.	CFN/SDT (50/50)	1.11	17.00	35	46.89
4.	CFN/SDT (60/40)	0.53	18.00	25	56.47
5.	CFN/SDT (80/20)	1.08	19.23	25	54.69

AC of all the briquette blends were high, caused by the carbonization of both feedstock before densification. Similar reason was reported by Severy et al. (2018), as the carbonization brings about loss of some appreciable amount of VM, leaving behind some volatile and non-volatile matter as AC of the produced briquette. Muazu and Stegemann (2017) also reported a close value of 19.6% AC as obtained in Table 3, compared to briquette CFN/SDT (80/20) at 19.23%. CFN/SDT (20/80) was observed to have the least value at 13.33%, with Cong et al. (2020) and Lela et al. (2015) having a bit lower. Adeleke et al. (2019) reported that coal have usually high AC value, and as reported herein, it increases as we move down the blends. High VM affects briquettes physical properties such as mechanical reliability, strength, durability and combustion efficiency (Adeleke et al., 2019).

The disclosed VM in Table 3, are moderately low from the produced blends of briquette; which is outrightly expected, as carbonization of the CFN and SDT would see most of the VM given off. Whereas studies from Sen et al. (2016) exposed closer values after their biomass materials have undergone thermal pretreatment – although, it was a bit higher than the one gotten in this study. CFN/SDT (50/50) blend presented the highest value of VM = 35% and a close value was revealed by Borowski et al. (2017). Ideally, FC composition is desired to be large, as it adds to the combustion value of a fuel (Akogun et al., 2020a). All the briquette blends presented high FC with CFN/SDT (20/80) being the greatest (at 66.09%). Similar huge values of high C content were reported in the literature (Manyuchi et al., 2018; Miao et al., 2019; Rejdak et al., 2020). Table 3 also reports CFN/SDT (50/50) as having the least FC = 46.89%, which could be as a result of the briquette blends not having a proper interlock (i.e., more room for material agglomeration) during densification. Ikelle and Ivoms (2018) revealed similar FC (%) from coal/corn cob briquette blend of 45% to > 65%. Bigger FC result in higher CV as published by Rajput and Thorat (2019) and Rapheal et al. (2018).

3.3. Briquette Blends Physical Characteristics Data

As contained in Table 4, D_{Bulk} of all the briquette blends ranges from 0.4000-0.6625 g/cm³ which falls within the values

delivered by Sen et al. (2016), and would also translate to better handling, transporting and intraparticle attraction. Highest D_{Bulk} at 0.6625 g/cm^3 for CFN/SDT (80/20) greatly indicate strength and good combustion properties (Kpalo et al., 2020). Still in Table 4, the D_{Rlx} reported is much higher than those gotten by Akpenpuun et al. (2020) – as a result of the compaction performed using hydraulic press for this work and the nature of the feedstock in terms of the optimum particle size used. D_{Rlx} for CFN/SDT (80/20) blend is also highest at 0.7501 g/cm^3 as expected, and may be linked to the optimum carbonization temperature of the CFN and SDT. Similar reason was reported by Akogun et al. (2020b).

Table 4: Physical Properties Determined

S/No.	Briquette Name Tag	D_{Bulk} (g/cm^3)	D_{Rlx} (g/cm^3)	HP (%)	SI (%)
1.	CFN/SDT (20/80)	0.4010	0.5952	91.33	92.13
2.	CFN/SDT (40/60)	0.5375	0.6919	93.11	93.21
3.	CFN/SDT (50/50)	0.4250	0.6473	95.40	94.47
4.	CFN/SDT (60/40)	0.4000	0.5438	96.64	96.51
5.	CFN/SDT (80/20)	0.6625	0.7501	98.19	98.66

Hydrophobic nature of the developed briquette blends increases with an increase in CFN mass ratio, due to the effectiveness in compaction and the binder used. The same briquette blend demonstrated greatest hydrophobicity relative to others. Yang et al. (2021) also revealed some briquettes that was made from carbonized/torrefied SDT, showing more resistance to moisture than untorrefied ones. The percentage gotten here is higher than that published in Abdullahi et al. (2021). CFN and SDT used here are at an optimal particle size distribution and is carbonized, thereby having lesser pore openings during the densification process. This imply that all the briquette blends can survive short-to-medium-term exposure to water, are of good strength and are highly durable. Greater than 90% SI is reported in Table 4 for all blends, implying the possession of excellent physical strength with high resistance to breakage when transporting. It also possesses a good mechanical stability, high durability, longevity and good combustion characteristics. In concordance with Akogun et al. (2020a) reporting over 90% SI, Kpalo et al. (2020) reported that the minimum SI of briquettes should be 90%. Briquette blend CFN/SDT (80/20) had the highest value of 98.66% which is synonymous to that identified by Ajiboye et al. (2016). It signifies good strength, resistance to breakage, better stability and endurance to mechanical and physical stress when compared with others.

3.4. Determined Briquette Blend Combustion Properties

IT = 2.15 min of CFN/SDT (80/20) was the highest due to the large ratio of CFN with characteristics mild volatility in the blend, as similar trend was revealed by Okonkwo et al. (2017) for coal/SDT blend briquettes (C50S50). On the other hand, CFN/SDT (40/60) possess the lowest IT at 1.37 min, which is attributed to the huge amount of SDT in the briquette blend. Such behavior was also obtained by Ajiboye et al. (2016) and implied quicker BT and lesser BR for such blend. In Table 5, BT demonstrates an increasing trend with rise in CFN ratio, which goes further to confirm the above reason given for the IT trend with SDT.

Table 5: Combustion Properties Realized for all Blends

S/No.	Briquette Name Tag	IT (min)	BT (min)	BR (g/min)
-------	--------------------	----------	----------	------------

1.	CFN/SDT (20/80)	1.50	46	0.43
2.	CFN/SDT (40/60)	1.37	48	0.42
3.	CFN/SDT (50/50)	1.55	40	0.50
4.	CFN/SDT (60/40)	1.40	50	0.40
5.	CFN/SDT (80/20)	2.15	55	0.36

It has a higher volatility thereby burning quicker, as similar development was reported by Elinge et al. (2019). CFN/SDT (50/50) blend BT = 40 min deviates a little from the trend, as a result of an imperfect compaction observed during densification – as that would see the briquette develop opened pores thereby influencing the BT, causing more air movement for combustion. BT for all the manufactured briquette blends appeared to be stable and near uniform because of the optimal particles size distribution adopted. Demirel and Bahadir (2018), Ndindeng et al. (2015) and Sutrisno et al. (2017) ascertain that smaller particle size influence BT in partial consonance with this study, since it encircles the optimal parameters. Table 5 shows burning time of the manufactured briquettes. Table 5 revealed that as the BT reduces, the CFN ratio increases while the SDT ratio decreases. Such is required as slow BR is most preferred for heating requirement (Elinge et al., 2019). BR was slower for CFN/SDT (80/20) at 0.36 g/min due to lesser pore opening in the briquette formation. It implied that it will take longer time to burn when compared with the remaining briquettes. This is desired as the period of burning is an imperative performance index in briquetting technology, as reported previously (Abdullahi et al., 2021; Aliyu et al., 2020).

3.5. AAS of Coal Samples

AAS analysis of the C, N and S contents of the demineralized CFN before and after washing for the series of reagents (HCl, NaOH, NaOH & HCl) used, is shown in Table 6. It was observed that C element amount increased for the combined 'NaOH + HCl' washing treatment compared to the other forms of treatment. It is due to the dual application of the reagents on the CFN and effective adsorption of the reagents to the body of the CFN, thereby exposing more of the C element while dissolving other undesired minerals, as reported by Behera et al. (2017). During the demineralization of high ash Indian coal by Sharma and Matsumura (2019), identical trend was revealed. Individual alkali and acid treatment also show an increase in the elemental C content from the unwashed to the washed sample. Despite it is below the combined ones, its characteristics is tied to more unwanted minerals dissolved in the solution. Behera and Chakraborty (2018) published similar trend when they applied NaOH and H_2SO_4 on a separate basis, as shown in Table 6.

Table 6: AAS Analysis of Demineralized CFN

S/No.	Sample ID	C (%)	N (%)	S (%)
1.	Washed HCl	60.39	0.022	0.12
2.	Washed NaOH	64.46	0.028	0.21
3.	Washed NaOH + HCl	70.39	0.017	0.02
4.	Unwashed HCl	52.35	0.087	0.18
5.	Unwashed NaOH	56.56	1.087	0.29
6.	Unwashed NaOH + HCl	55.37	0.854	0.18

N and S elements generate hazardous substances by reacting with other gasses in the form of NO_x and SO_x contained in briquette during combustion, and the maximum allowable S and N content for briquette is 5%; as recommended by the Thailand Industrial Standards and reported by Aliyu et al. (2020). However, the one presented herein is within the standard and can be burnt without any pollution concern. N and S compositions reduced for all the reagents used for unwashed and washed samples. Simply because the reaction and desorption of the N and S content in the raw CFN with the

solutions (alkali, acid & alkali-acid) is in agreement with Fedorova et al. (2018).

3.6. Ultimate Analysis Report and CV

Table 7 show that C content dominated the briquette blends, which is attributed to the demineralization effect carried out on the CFN, where most of the unwanted minerals (S, N, Al, Na, Mg, K, Si, Ca & Mn) is dissolved off. These minerals cause corrosion, fouling, SO_x/NO_x emissions reduction in gross CV of briquette. Adekunle et al. (2020) realized and reported similar occurrences. Also, Rahman et al. (2017) pointed out same process of dissolution of such minerals by alkali-acid demineralization treatments for achieving clean coal samples.

Table 7: Developed Briquette Blends CHNSO Amounts and CV Percent

Briquette Blend	C (%)	H (%)	N (%)	S (%)	O (%)	CV (MJ/kg)
CFN/SDT (20/80)	66.45	3.98	0.61	0.20	28.38	25.27
CFN/SDT (40/60)	68.41	3.82	2.61	0.30	24.14	25.95
CFN/SDT (50/50)	69.37	4.55	0.64	0.11	24.33	27.15
CFN/SDT (60/40)	69.89	4.18	0.74	0.10	24.66	26.95
CFN/SDT (80/20)	70.90	3.95	0.60	0.07	23.47	27.22

O is a little bit high, but is in the required value, as these amounts will not affect combustion characteristics of the briquette blends. Kumar et al. (2017) reported close values after demineralization but recorded good burning history of their produced briquettes. S, N and other ash forming minerals presented here, are in low concentrations due to the demineralization effect. In the literature, briquette blends with good combustion characteristics, denser briquettes, cleaner and purer briquette blend samples, were presented (Aditya et al., 2018; Bilen, 2019; Fedorova et al., 2018; Isobaev et al., 2019; Mketi et al., 2017; Rahman et al., 2017; Rizkiana et al., 2020). Column 7 of Table 7 houses the CV of the developed briquette blends. Normally, high CV is required and in this study, as well as in Manyuchi et al. (2018), the reason for the high heating value was due to the blends and binder employed in the briquette manufacturing. Another reason for the high CV in briquette is linked to the fact that carbonized or torrefied CFN, SDT and other briquette feedstocks, presents them with reduced VM and a decreased MC which provides balance, easy burning and a good CV. Akogun et al. (2020b) reported and linked similar scenario with their produced briquettes. It is important to state that thermal (carbonization) treatment of CFN and SDT influence C content and the CV of briquette, as in Song et al. (2019). CV reported in this research work is in conformity with literature report (Borowski et al., 2017; Burenina et al., 2019; Trubetskaya et al., (2019).

3.7. Coal SEM and XRD

In the un-demineralized coal, clear large and spreaded luminous materials indicating the presence of inorganic minerals such as S, N, Si, Al, K, Na, Mg, Mn and Ca, was revealed by SEM. Pore opening seemed to be absent in its structural and physical outlook, as shown in Figure 3a. Figure 3b show tinier features of the demineralized coal while Figure 3c shows that the best performing briquette blend (i.e., CFN/SDT (80/20)) had good mechanical interlock. This behavior is solely attributed to the effect of the Gum Arabic binder explored with the carbonized SDT blend.

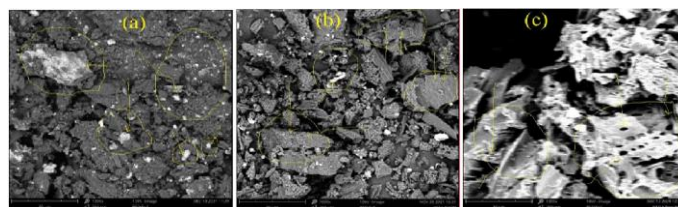


Figure 3: SEM Morphology of (a) Un-demineralized Coal, (b) Demineralized coal and (c) CFN/SDT (80/20) Best Performing Briquette Blend

Bigger pore opening on the body of the developed briquette blend will allow air transport during combustion with total absence of luminous minerals, further verifying the AAS analysis presented in Table 6. XRD analysis of the un-demineralized coal presented by Figure 4a contains largely kaolinite (chemically known as aluminosilicate- $Al_2Si_2O_5(OH)_4$) and quartz crystalline free silica (SiO_2) minerals. Peak intensities at $2\theta = 12.4810^\circ$, 24.9377° and 26.7308° were seen to have declined to 12.4710° , 24.8757° and 26.6725° , respectively, in Figure 4b, which is that of demineralized coal using NaOH-HCl reagents solutions.

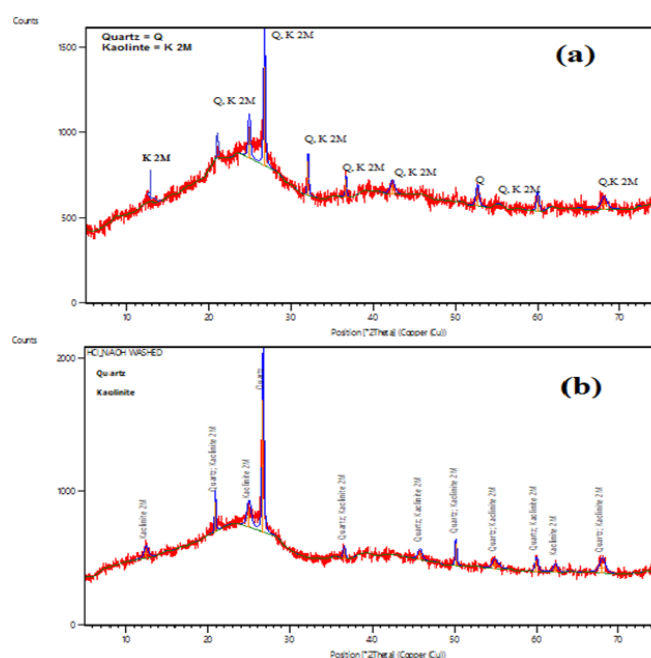


Figure 4: XRD Analysis of (a) Un-demineralized and (b) Demineralized Coal Sample

It further confirms the removal of the inorganic minerals contained in the un-demineralized coal and the AAS result in Table 6. For the manufactured briquette blends, similar trend was reported by Aditya et al. (2018), although there are remaining kaolinite and quartz minerals in the demineralized coal, which may be due to the unliberated silica and alumina contained in the pores of the coal. Barma et al. (2018) stated similar reason in their published work. The weak peak at $2\theta = 42.2966^\circ$ for the un-demineralized coal is attributed by (101) plane reflection of graphite (Manoj, 2016).

3.8. FTIR Functional Groups and EDXRF

FTIR analysis of the un-demineralized and demineralized coal is carried out so as to analyze the functional groups present in the samples, as shown in Figure 5. The peaks absorbance band at 1039 cm^{-1} for the un-demineralized coal in Figure 5a represent Si-O-Si stretching group and signifies the presence of inorganic minerals of quartz (silica) and kaolinite (alumina) Ghorai et al. (2019). It is also known as the mineral band. In

Behera and Chakraborty (2018) and as confirmed by SEM and XRD analysis, the band at 1369 cm^{-1} and 1580 cm^{-1} signifies the coal lignin content (Okoro et al., 2018) and 1887 cm^{-1} and 2081 cm^{-1} shows the existence of aliphatic and aromatic CH groups (Barma et al., 2018). The peaks at 2844 cm^{-1} and 2918 cm^{-1} are responsible for symmetric $\text{CH}_2\text{-CH}_3$ vibrations (Behera and Chakraborty, 2018) and asymmetric CH_2 vibrations (Ghorai et al., (2019).

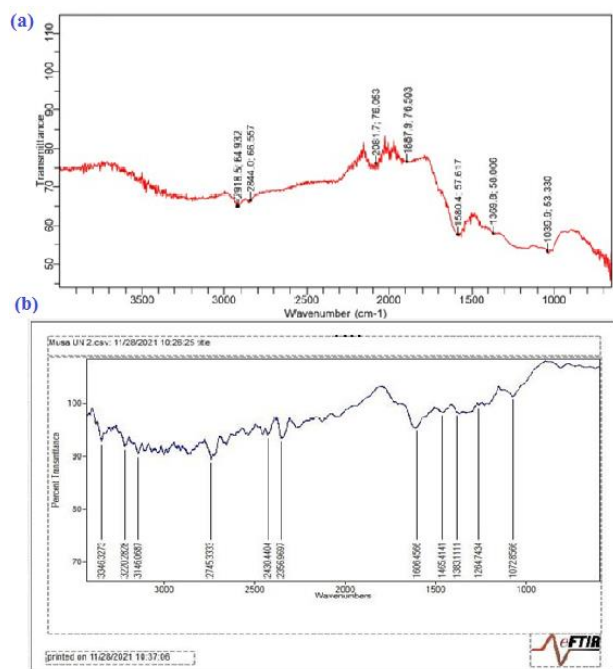


Figure 5: FTIR Analysis of (a) Un-demineralized and (b) Demineralized Coal Sample

Figure 5b is the FTIR peaks for the demineralized coal and a shift in peak from the un-demineralized coal was observed. At 1039 and 1580 cm^{-1} , respectively, Si-O-Si group and lignin content ceases to exist, indicating that quartz and kaolinite inorganic minerals demineralization has taken effect. Ghorai et al. (2019) reported similar trend, as new peaks were seen manifesting for demineralized coal sample. The peak at 1264 cm^{-1} is due to C-O vibrations (Ghorai et al., 2019). Absorption band at 1465 cm^{-1} shows occurrence of ethylene and methyl groups in the demineralized coal sample (Okoro et al., 2018). Peak at 1606 cm^{-1} is a strong absorption band showing aromatic C=C stretching (Barma et al., 2018; Behera and Chakraborty, 2018; Okoro et al., 2018). Other peaks band at 2356 , 2430 , 2745 cm^{-1} and 3146 , 3220 , 3346 cm^{-1} indicates strong aliphatic and hydroxyl groups which designates improvement in C, H and O values of the demineralized coal samples, as reported by Barma et al. (2018). The EDXRF analysis is presented in Figure 6.

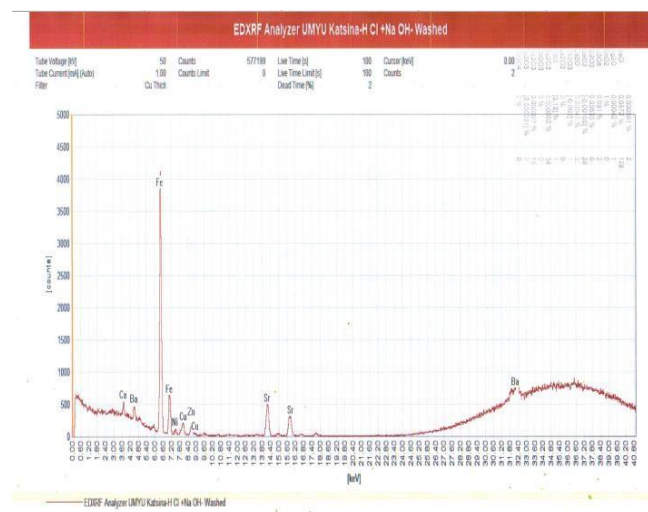


Figure 6: EDXRF Analysis of the Demineralized Coal

S and other mineral content shown in Figure 6 of the EDXRF analysis for demineralized coal are less, while some are beyond the detection level (Rimmer and Wei, 2018). This is due to the demineralization process effected on the raw coal sample. S content reported by Zhao et al. (2015) and Zhang et al. (2016) is higher than the one presented in this work after demineralization; simply because they only carryout demineralization using acid pretreatment. The reason behind the reduction of these element on the demineralized coal is due to their absorption from the surface of the coal to the solution of the reagent (Yang et al., 2019). Other elemental compositions are shown in Table 8.

Table 8: EDXRF Elemental Analysis of the Demineralized Coal (HCl + NaOH – Washed)

Element	Concentration (%)	Peak (cps/mA)
Fe	1.0768	5719
Si	2.538	400
Al	0.889	26
Mg	[0.14]	0
P	0.0170	9
S	0.6494	1026
Ti	0.2035	1221
Mn	0.1655	646
Ca	0.9026	1887
K	0.0603	76
Cu	0.02210	88
Zn	0.02898	197
Cr	0.00920	105
V	0.00520	61
As	[0.0005]	0
Pb	0.00229	1
Rb	0	0
Ga	0.00060	11
Ni	0.00631	44
Cl	0.02323	34
Zr	[-0.01000]	18
Ta	0.0035	5
W	0.096	13
Br	0.000320	1
Sr	[0.012]	45
Ce	1.40	4
Th	0.00067	0
Y	0.001361	3
Nb	0.06015	2
I	0.000589	2
Ag	0.00045	1

3.9. Performance Evaluation of the Developed Briquette Blends with Cooking Stove

WBT in Table 9 show that firewood had the highest BT of 17 min followed by charcoal (14 min). Davies et al. (2013) reported similar charcoal BT while reporting lesser firewood BT, in addition to Brenda et al. (2017) who reported greater BT for firewood and lesser for charcoal. This is firstly due to their low CV. Secondly, they are not compacted as briquettes, as high CV enable higher energy to be given off within the solid fuel (Lubwama et al., 2019). Also, this is the case with the other briquette blends. CFN/SDT (80/20) briquette blend presented the shortest BT of 7 min, because it is the briquette with the highest CV. The thermal efficiency of the developed briquette blends and stove in Table 9 was best when the solid fuel in use is the developed briquette blends, where they ranged from 63 to > 80%. This value is in the same range obtained by Oyejide et al. (2019) and Wang et al. (2019) due to the anthill and clay insulation applied, even much higher than those reported by Bantu et al. (2018), Sari et al. (2020) and Verma and Shukla (2019).

Table 9: Solid Fuel Performance and WBT

S/No.	Solid Fuel Name	WBT (min)	PHU (%)
1.	Firewood	17	38
2.	Charcoal	14	41
3.	CFN/SDT (20/80)	11	63
4.	CFN/SDT (40/60)	10	71
5.	CFN/SDT (50/50)	8	80
6.	CFN/SDT (60/40)	9	78
7.	CFN/SDT (80/20)	7	86

It means that the developed stove will perform better when the solid fuel to be used in it is CFN and SDT briquette blends than the conventional firewood and charcoal, as they presented lower percentages. This could directly be related to lower CV of charcoal and firewood, as lesser CV will mean lesser heat energy recovery of a solid fuel. Verma and Shukla (2019) mentioned that, it will produce disturbing smoke during the course of the test, compared to all other briquette blends producing lesser non-disturbing smoke. It has been sufficiently proven that they are better replacement of firewood and charcoal utilization for domestic cooking or heating applications. In this study, the firewood PHU determined, had greater value while that of charcoal was close to that reported by Davies et al. (2013), as a result of the anthill/clay insulation.

CONCLUSION

Likelihood of developing briquette stove from locally sourced materials in Nigeria have been successfully examined. The developed briquette blends' proximate, physical, ultimate and thermal properties indicate that CFN/SDT (80/20) blend was the best performing briquette. An AAS analysis performed show values of N and S that is less, but having a very high C content. SEM micrograph showed that almost all the shiny large materials are lost, with only traces left as observed in some increased pore openings on the surface of the demineralized coal samples. That of the briquette blend showed available pore opening which will allow air transport during combustion with clear mechanical interlock indicating good bonding effect of the binder used. XRD spectra for the undemineralized coal at $2\theta = 26.7308^\circ$ was seen to have reduced to $2\theta = 26.6725^\circ$ for the demineralized coal. FTIR analysis revealed a strong absorption band at 1606 cm^{-1} showing aromatic C=C stretching which indicated the formation of carbonaceous compounds in the composite used for the demineralized coal. Amount of N, S and other unwanted minerals characterized by EDXRF for demineralized coal were within the threshold specified by Thailand Industrial Standards (< 5%). WBT result of the produced briquette blend was more

favorable than the conventional fuels where CFN/SDT (80/20) blend had the shortest BT and thus, is directly proportional to the briquette's highest CV. The percentage heat utilized otherwise called thermal efficiency of the briquette blends were much higher, with CFN/SDT (80/20) blend posing thermal efficiency of 86% without smoke nuisance compared to the conventional fuels at 38 and 41%, respectively (producing black smoke believed to be CO emissions). It is evident that the stove developed is more environmentally friendly and can be adopted both in rural and urban settings in Nigeria. Further characterization to study heat sensitivity of the briquette blends using thermo-gravimetric analysis (TGA) should be carried out.

Data Availability

No data were used to support this study.

How to Cite: Musa Alhassan et al. (2024). Eco-Friendly Cooking Solutions: Design and Evaluation of Stoves and Briquettes Made from Coal Fines and Sawdust, *Abhath Journal of Basic and Applied Sciences*, 3(1), 27-39. <https://doi.org/10.59846/ajbas.v3i1.640>

References

- [1] Abdullahi, L., Abubakar, M., & Ndagi, B. (2021). Effect of compaction pressure and biomass type (rice husk and sawdust) on some physical and combustion properties of briquettes. *Arid Zone Journal of Engineering, Technology & Environment*, 17(1), 61–70. <https://azojete.com.ng/index.php/azojete/article/view/404>
- [2] Adeleke, A A, Odusote, J. K., Ikubanni, P. P., Orhadahwe, T. A., & Lasode, O. A. (2021). Ash analyses of bio-coal briquettes produced using blended binder. *Scientific Reports*, 1–9. <https://doi.org/10.1038/s41598-020-79510-9>
- [3] Adeleke, A A, Odusote, J. K., Lasode, O. A., Ikubanni, P. P., Malathi, M., & Paswan, D. (2019). Densification of coal fines and mildly torrefied biomass into composite fuel using different organic binders. *Heliyon*, 5, 1–7. <https://doi.org/10.1016/j.heliyon.2019.e02160>
- [4] Aditya, A., Suresh, A., Sriramoju, S. K., Dash, P. S., Pati, S., Padmanabhan, N. P. H., Suresh, A., Sriramoju, S. K., Dash, P. S., & Pati, S. (2018). Optimization study of sodium hydroxide consumption in the coal demineralization process. *Mineral Processing and Extractive Metallurgy Review*, 1–8. <https://doi.org/10.1080/08827508.2017.1415208>
- [5] Ajiboye, T., Abdulkareem, S., & Anibijuwon, A. O. Y. (2016). Investigation of mechanical properties of briquette product of sawdust-charcoal as a potential domestic energy source. *Journal of Applied Science and Environmental Management*, 20(4), 1179–1188. <http://dx.doi.org/10.4314/jasem.v20i4.34>
- [6] Akogun, Ayodeji, Opeyemi, Waheed, Adekojo, Mufutau, Olasunkanmi, & Salami. (2020a). Physical and combustion indices of thermally treated cornhusk and sawdust briquettes for heating applications in Nigeria. *Journal of Natural Fibers*, 478, 1–17. <https://doi.org/10.1080/15440478.2020.1764445>
- [7] Akogun, O., A, Waheed, M. A., Ismaila, S. O., & Olawale, U. (2020b). Co-briquetting characteristics of cassava peel with sawdust at different torrefaction pretreatment conditions. *Energy Sources, Part A: Recovery, Utilization, and Environmental Effects*, 1–19. <https://doi.org/10.1080/15567036.2020.1752333>
- [8] Akolgo, Ayine, G., Awafo, A. E., Essandoh, Osei, E., Owusu, Achaw, P., Uba, Felix, Adu-poku, & A, K. (2021). Assessment of the potential of charred briquettes of sawdust, rice and coconut husks: Using water boiling and user acceptability tests. *Scientific African*, 12, 1–8. <https://doi.org/10.1016/j.sciaf.2021.e00789>

- [9] Akpenpuun, T., Ra, S., Ao, A., Om, A., J, S., & M, D. (2020). Physical and combustible properties of briquettes produced from a combination of groundnut shell, rice husk, sawdust and wastepaper using starch as a binder. *Journal of Applied Science and Environmental Management*, 24(1), 171–177. <http://dx.doi.org/10.4314/jasem.v24i1.25>
- [10] Aliyu, M., Mohammed, I. S., Usman, M., Musa, S., & Igbetua, I. J. (2020). Production of composite briquettes (orange peels and corn cobs) and determination of its fuel properties. *Agricultural Engineering International*, 22(2), 1–13. <http://www.cigrjournal.org>
- [11] Anna Brunerová, Roubík, H., & Brožek, M. (2018). Bamboo fiber and sugarcane skin as a bio- briquette fuel. *Energies*, 1–20. <https://doi.org/10.3390/en11092186>
- [12] Bantu, A. A., Nuwagaba, G., Kizza, S., & Turinayo, Y. K. (2018). Design of an improved cooking stove using high density heated rocks and heat retaining techniques. *Journal of Renewable Energy*, 1–10. <https://doi.org/https://doi.org/10.1155/2018/9620103>
- [13] Barma, S. D., Sathish, R., & Baskey, P. K. (2018). Ultrasonic-assisted cleaning of Indian low- grade coal for clean and sustainable energy. *Journal of Cleaner Production*, 1–36. <https://doi.org/10.1016/j.jclepro.2018.06.030>
- [14] Behera, S. K., & Chakraborty, S. (2018). Demineralization mechanism and influence of parameters on high ash Indian coal by chemical leaching of acid and alkali solution. *International Journal of Coal Science & Technology*, 5(2), 142–155. <https://doi.org/10.1007/s40789-018-0208-3>
- [15] Behera, S. K., Chakraborty, S., & Meikap, B. C. (2017). Chemical demineralization of high ash Indian coal by using alkali and acid solutions. *Fuel*, 196, 102–109. <https://doi.org/10.1016/j.fuel.2017.01.088>
- [16] Bello, R. S., & Onilude, M. A. (2020). Physico-mechanical characteristics of high density briquettes produced from composite sawdust. *Journal of Applied Science and Environmental Management*, 24(5), 779–787. <https://doi.org/https://dx.doi.org/10.4314/jasem.v24i5.8>
- [17] Bilen, M. (2019). Proximate and ultimate analysis before and after physical & chemical demineralization. *Earth and Environmental Science*, 362, 1–8. <https://doi.org/10.1088/1755-1315/362/1/012092>
- [18] Bonsu, Osei, Betty, Takase, Mohammed, Mantey, & Jones. (2020). Preparation of charcoal briquette from palm kernel shells: case study in Ghana. *Heliyon*, 6(10), 1–8. <https://doi.org/10.1016/j.heliyon.2020.e05266>
- [19] Borowski, G., Stępniewski, W., & Wójcik-oliveira, K. (2017). Effect of starch binder on charcoal briquette properties. *International Agrophysics*, 31, 571–574. <https://doi.org/10.1515/intag-2016-0077>
- [20] Brenda, M. G., Innocent, E. E., Daniel, O., & Abdu, Y. A. (2017). Performance of biomass briquettes as an alternative energy source compared to wood charcoal in Uganda. *International Journal of Scientific Engineering and Science*, 1(6), 55–60.
- [21] Brunerov, Anna, Roub, Hynek, Brožek, Milan, Haryanto, Agus, Hasanudin, & Udin. (2019). Valorization of bio-briquette fuel by using spent coffee ground as an external additive. *Energies*, 1–15. <https://doi.org/10.3390/en13010054>
- [22] Brunerová, A., Malatřák, J., Müller, M., Valášek, P., & Roubík, H. (2017). Tropical waste biomass potential for solid biofuels production. *Agronomy Research*, 15(2), 359–368.
- [23] Burenina, O. N., Nikolaeva, L. A., & Solovev, T. M. (2019). Development of technologies for processing large-tonnage accumulations of oil sludge and wood waste with obtaining binders to improve the quality of household briquetted fuel based on brown coal. *IOP Conference Series: Earth and Environmental Science*, 272(2), 1–6. <https://doi.org/10.1088/1755-1315/272/2/022146>
- [24] Okonkwo Ugochukwu C, O. U., Agu Chukwuemerie N, A. C., Samuel, A., & Sinebe Jude E, S. J. (2017). Proximate analysis and performance evaluation of selected blends of biomass briquettes. *Journal of Engineering and Applied Sciences*, 10, 144–161.
- [25] Dai, S., & Finkelman, R. B. (2017). Coal as a promising source of critical elements: Progress and future prospects. *International Journal of Coal Geology*, 1–37. <https://doi.org/10.1016/j.coal.2017.06.005>
- [26] Davies, R. M., Davies, O. A., & Mohammed, U. S. (2013). Combustion characteristics of traditional energy sources and water hyacinth briquettes. *International Journal of Scientific Research in Environmental Sciences (IJSRES)*, 1(7), 144–151. <http://dx.doi.org/10.12983/ijres-2013-p144-151>
- [27] Demirel, & Bahadir. (2018). Effect of particle size on surface smoothness of bio-briquettes produced from agricultural residues. *Manufacturing Technology*, 1–7. <https://doi.org/10.21062/ujep/170.2018/a/1213-2489/MT/18/5/742>
- [28] Elehinafe, F B, Okedere, O. B., & Odunlami, O. (2019). Proximate analysis of the properties of some southwestern Nigeria sawdust of different wood species. *International Journal of Civil Engineering and Technology (IJCIET)*, 10(3), 51–59.
- [29] Elehinafe, Francis B, Okedere, O. B., Fakinle, B. S., & Jacob, A. (2017). Assessment of sawdust of different wood species in Southwestern Nigeria as source of energy. *Energy Sources, Part A: Recovery, Utilization, and Environmental Effects*, 1–5. <https://doi.org/10.1080/15567036.2017.1384869>
- [30] Elinge, C. ., Birnin-Yauri, A. ., Senchi, D. ., A.R, I., Ajakaye, J., Yusuf, A., & Abubakar, R. . (2019). Studies on the combustion profile of briquettes produced from carbonized rice husk using different binders at moderate temperature and die pressure. *International Journal of Advanced Academic Research*, 5(3), 70–77.
- [31] Fedorova, N. I., Dudnikova, Y. N., & Zykov, I. Y. (2018). Influence of the demineralization of naturally oxidized coal on sorbent texture. *Coke and Chemistry*, 61(8), 297–300. <https://doi.org/10.3103/S1068364X18080045>
- [32] Finkelman, R. B., Dai, S., & French, D. (2019). The importance of minerals in coal as the hosts of chemical elements: A review. *International Journal of Coal Geology*, 212, 1–17. <https://doi.org/10.1016/j.coal.2019.103251>
- [33] Francis, O. (2015). Evaluation of the effect of palm oil mill sludge on the properties of sawdust briquette. *Renewable and Sustainable Energy Reviews*, 52, 1749–1758. <https://doi.org/10.1016/j.rser.2015.08.001>
- [34] Ghorai, S., Ghosh, B., Chandaliya, V. K., Singh, R., Dash, P. S., & Mal, D. (2019). Difference in structural chemistry of non-coking and coking coal using acid treatment demineralization technique. *International Journal of Coal Preparation and Utilization*, 1–21. <https://doi.org/10.1080/19392699.2019.1664482>
- [35] Ikelle, I. I., & Ivoms, O. S. P. (2018). Determination of the heating ability of coal and corn cob briquettes. *Journal of Applied Chemistry (IOSR-JAC)*, 7(2), 77–82. <https://doi.org/10.9790/5736-07217782>
- [36] Isobaev, M. D., Davlatnazarova, M. D., & Mingboev, S. A. (2019). Acid demineralization and activation of coal sorbents. *Solid Fuel Chemistry*, 53(3), 172–174. <https://doi.org/10.3103/S0361521919030042>

- [37] Jaya, T., PhD, Engineer, D. S., Fillerup, Eric, & Falls, I. (2020). In the field briquetting characteristics of woody and herbaceous biomass blends: Impact on physical properties, chemical composition, and calorific value. *Biofuels, Bioproducts and Biorefining.*, 1–20. <https://doi.org/10.1002/bbb.2121>
- [38] Khatib, M. I., Ahmed, R. Z., Uddin, M. S., Abdul Rahman, M., Shareef, M. R., Akber, S., Khan, M., & Shaikh, S. (2020). Design and fabrication of 5 ton hydraulic press machine. *International Journal of Scientific Research in Science, Engineering and Technology*, 7(2), 1–11. <https://doi.org/10.32628/ijrsrset207210>
- [39] Kpalo, Yusuf, Sunday, Zainuddin, Faiz, Mohamad, Manaf, Abd, & Latifah. (2020). Production and characterization of hybrid briquettes from corncobs and oil palm trunk bark under a low pressure densification technique. *Sustainability*, 1–16. <https://doi.org/10.3390/su12062468>
- [40] Kumar, A., Singh, A. K., Singh, P. K., Singh, A. L., & Jha, M. K. (2017). Demineralization study of high ash Permian coal with *Pseudomonas mendocina* strain B6-1: A case study of South Karanpura coalfield, Jharkhand, India. *Energy and Fuels*, 1–23. <https://doi.org/10.1021/acs.energyfuels.7b02562>
- [41] Lela, B, Barišic, M., & Nizetic, S. (2015). Cardboard/sawdust briquettes as biomass fuel: physical – mechanical and thermal characteristics. *Waste Management*, 1–10. <https://doi.org/10.1016/j.wasman.2015.10.035>
- [42] Lubwama, M., Yiga, V. A., & Lubwama, H. N. (2020). Effects and interactions of the agricultural waste residues and binder type on physical properties and calorific values of carbonized briquettes. *Biomass Conversion and Biorefinery*, 1–21. <https://doi.org/10.1007/s13399-020-01001-8>
- [43] Lubwama, M., Yiga, V. A., Muhairwe, F., & Kihedu, J. (2019). Physical and combustion properties of agricultural residue bio-char bio-composite briquettes as sustainable domestic energy sources. *Renewable Energy*, 1–37. <https://doi.org/10.1016/j.renene.2019.10.085>
- [44] Mandal, S., Kumar, G. V. P., & Tanna, T. K. B. H. R. (2018). Briquetting of Pine Needles (*pinus roxburgii*) and their physical, handling and combustion properties. *Waste and Biomass Valorization*, 1–10. <https://doi.org/10.1007/s12649-018-0239-4>
- [45] Manoj, B. (2016). A comprehensive analysis of various structural parameters of Indian coals with the aid of advanced analytical tools. *International Journal of Coal Science & Technology*, 3, 1–13. <https://doi.org/10.1007/s40789-016-0134-1>
- [46] Manouchehrinejad, M., Yue, Y., Armond, R., Morais, L. De, Macedo, L., & Souza, O. (2018). Densification of thermally treated energy cane and napier grass. *Bioenergy Research*, 1–13. <https://doi.org/10.1007/s12155-018-9921-4>
- [47] Manyuchi, M. M., Mbohwa, C., & Muzenda, E. (2018). Value addition of coal fines and sawdust to briquettes using molasses as a binder. *South African Journal of Chemical Engineering*, 26, 70–73. <https://doi.org/10.1016/j.sajce.2018.09.004>
- [48] Massaro, M. M., Son, S. F., & Groven, L. J. (2014). Mechanical, pyrolysis, and combustion characterization of briquetted coal fines with municipal solid waste plastic (MSW) binders. *Fuel*, 115, 62–69. <https://doi.org/10.1016/j.fuel.2013.06.043>
- [49] Miao, Z., Zhang, P., Li, M., Wan, Y., & Meng, X. (2019). Briquette preparation with biomass binder. *Energy Sources, Part A: Recovery, Utilization and Environmental Effects*, 1–11. <https://doi.org/10.1080/15567036.2019.1682722>
- [50] Mketi, N., Nomngongo, P. N., & Ngila, J. C. (2017). Rapid total sulphur reduction in coal samples using various dilute alkaline leaching reagents under microwave heating: preventing sulphur emissions during coal processing. *Environmental Science Pollution Research*, 1–7. <https://doi.org/10.1007/s11356-017-9632-y>
- [51] Mohammed, Y. S., Mustafa, M. W., Bashir, N., Ogundola, M. A., & Umar, U. (2014). Sustainable potential of bioenergy resources for distributed power generation development in Nigeria. *Renewable and Sustainable Energy Reviews*, 34, 361–370. <https://doi.org/10.1016/j.rser.2014.03.018>
- [52] Moreno, A. I., Font, R., & Conesa, J. A. (2016). Physical and chemical evaluation of furniture waste briquettes. *Waste Management*, 1–8. <https://doi.org/10.1016/j.wasman.2016.01.048>
- [53] Motghare, K. A., Labhsetwar, N. K., Rathod, A. P., Waghmare, S. S., & K.L.Wasewar. (2015). Performance Evaluation and Heat transfer studies on Biomass Gasifier cook-stove. *International Journal of Application or Innovation in Engineering & Management (IJAIEM)*, 4(5), 352–361.
- [54] Muazu, R. I., & Stegemann, J. A. (2017). Biosolids and microalgae as alternative binders for biomass fuel briquetting. *Fuel*, 194, 339–347. <https://doi.org/10.1016/j.fuel.2017.01.019>
- [55] Musa, U., Ishaq, K., Onoduku, & Shehu, U. (2016). Characterization and ash chemistry of selected Nigerian coals for solid fuel combustion. *Petroleum and Coal*, 56(6), 1–10.
- [56] Ndingeng, S. A., Mbassi, J. E. G., Mbacham, W. F., Manful, J., Graham-acquaah, S., Moreira, J., Dossou, J., & Futakuchi, K. (2015). Quality optimization in briquettes made from rice milling by-products. *Energy for Sustainable Development*, 29, 24–31. <https://doi.org/10.1016/j.esd.2015.09.003>
- [57] Nwabue, F. I., Unah, U., & Itumoh, E. J. (2017). Production and characterisation of smokeless bio-coal briquettes incorporating plastic waste materials. *Environmental Technology & Innovation*, 1–26. <https://doi.org/10.1016/j.eti.2017.02.008>
- [58] Ogunwusi, A. A. (2014). Wood waste generation in the forest industry in Nigeria and prospects for its industrial utilization. *Civil and Environmental Research*, 6, 62–70. <https://core.ac.uk/download/pdf/234677849.pdf>
- [59] Okino, J., Komakech, A. J., Wanyama, J., Ssegane, H., Olomo, E., & Omara, T. (2021). Performance characteristics of a cooking stove improved with sawdust as an insulation material. *Journal of Renewable Energy*, 1–12. <https://doi.org/https://doi.org/10.1155/2021/9969806>
- [60] Okoro, S. E., Asadu, C. O., & Maxwell, I. (2018). Demineralization of Enugu coal: effect of acid type and acid concentration. *Journal of the Chinese Advanced Materials Society*, 6(4), 573–604. <https://doi.org/10.1080/22243682.2018.1522971>
- [61] Onoduku, U. S. (2014). Chemistry of maiganga coal deposit, upper benue trough, northeastern Nigeria. *Journal of Geosciences and Geomatics*, 2(3), 80–84. <https://doi.org/10.12691/jgg-2-3-2>
- [62] Oyejide, O. J., Okwu, M. O., & Tartibu, L. K. (2019). Adaptive design and development of a modular water hyacinth briquette stove. *Energy Sources, Part A: Recovery, Utilization, and Environmental Effects*, 1–19. <https://doi.org/10.1080/15567036.2019.1675808>
- [63] Patil, G. (2019). The possibility study of briquetting agricultural wastes for alternative energy. *Indonesian*

- Journal of Forestry Research*, 6(2), 133–139. <https://doi.org/10.20886/ijfr.2019.6.2.133-139>
- [64] Pontevedra, V., Kongprasert, N., Wangphanich, P., Jutilartavorn, A., Kongprasert, N., Wangphanich, P., & Jutilartavorn, A. (2019). Charcoal briquettes from madan wood waste as an alternative energy in Thailand. *Procedia Manufacturing*, 30, 128–135. <https://doi.org/10.1016/j.promfg.2019.02.019>
- [65] Rahaman, S. A., & Salam, P. A. (2017). Characterization of cold densified rice straw briquettes and the potential use of sawdust as binder. *Fuel Processing Technology*, 158, 9–19. <https://doi.org/10.1016/j.fuproc.2016.12.008>
- [66] Rahman, M., Pudasainee, D., & Gupta, R. (2017). Review on chemical upgrading of coal: Production processes, potential applications and recent developments. *Fuel Processing Technology*, 158, 35–56. <https://doi.org/10.1016/j.fuproc.2016.12.010>
- [67] Rajput, S. P., & Thorat, B. N. (2019). Recovered polyvinyl alcohol as an alternative binder for the production of metallurgical quality coke breeze briquettes. *International Journal of Coal Preparation and Utilization*, 1–11. <https://doi.org/10.1080/19392699.2019.1619558>
- [68] Rapheal, I. A., Moki, E. C., Gusau, H. L., & Abimbola, A. I. (2018). Effect of binder on physico-chemical properties of fuel briquettes produced from watermelon peels. *AASCIT Journal of Energy*, 5(2), 1–6. <http://www.aascit.org/journal/energy>
- [69] Rejdak, M., Robak, J., Czardybon, A., Ignasiak, K., & Fudała, P. (2020). Research on the production of composite fuel on the basis of fine-grained coal fractions and biomass—the impact of process parameters and the type of binder on the quality of briquettes produced. *Minerals*, 10(1), 1–12. <https://doi.org/10.3390/min10010031>
- [70] Rimmer, S., & Wei, Q. (2018). Acid solubility and affinities of trace elements in the high-Ge coals from Wulantuga (Inner Mongolia) and Lincang (Yunnan Province), China. *International Journal of Coal Geology*, 178, 39–55. <https://doi.org/10.1016/j.coal.2017.04.011>
- [71] Rizkiana, J., Ananda, R. F., Kamilah, N., & Nur, G. A. (2020). The effect of demineralization towards gasification performance of low-rank coal. *Materials Science and Engineering*, 823, 1–9. <https://doi.org/10.1088/1757-899X/823/1/012023>
- [72] Sajadi, A., Dashti, A., Ahmadijokani, F., Hu, J., & Mohammadi, A. H. (2021). Estimation of higher heating values (HHVs) of biomass fuels based on ultimate analysis using machine learning techniques and improved equation. *Renewable Energy*, 179, 550–562. <https://doi.org/10.1016/j.renene.2021.07.003>
- [73] Sari, E., Khatab, U., Rahman, E. D., Panindi, A., & Andriyati, E. (2020). Design of biomass briquette stoves: performance based on mixed of durian bark, coconut shell and palm shells as materials of bio briquette. *Materials Science and Engineering*, 990, 1–8. <https://doi.org/10.1088/1757-899X/990/1/012013>
- [74] Sen, R., Wiwatpanyaporn, S., & Annachhatre, A. P. (2016). Influence of binders on physical properties of fuel briquettes produced from cassava rhizome waste. *International Journal Environment and Waste Management*, 17(2), 158–175. <http://dx.doi.org/10.1504/IJEW.2016.076750>
- [75] Severy, M. A., Chamberlin, C. E., Eggink, A. J., & Jacobson, A. E. (2018). Demonstration of a pilot-scale plant for biomass torrefaction and briquetting. *Waste to Wisdom*, 34(1), 85–98. <http://dx.doi.org/10.13031/aea.12376>
- [76] Sharma, A., & Matsumura, A. (2019). A comparative study on demineralization of coals by acid- washing and solvent-extraction methods for low temperature catalytic coal gasification application. *Carbon Resources Conversion*, 2(3), 175–181. <https://doi.org/10.1016/j.crcon.2019.09.001>
- [77] Song, Q., Zhao, H., Jia, J., Yang, L., Lv, W., Gu, Q., & Shu, X. (2019). Effects of demineralization on the surface morphology, microcrystalline and thermal transformation characteristics of coal. *Journal of Analytical and Applied Pyrolysis*, 1–12. <https://doi.org/10.1016/j.jaap.2019.104716>
- [78] Sutrisno, Anggono, W., Suprianto, F. D., Kasrun, A. W., & Siahaan, I. H. (2017). The effects of particle size and pressure on the combustion characteristics of cerbera manghasleaf briquettes. *Journal of Engineering and Applied Sciences*, 12, 1–18.
- [79] Tom, S., Shuma, M. R., Madyira, D. M., & Kaymakci, A. (2016). Performance Testing of a Multi-layer Biomass Briquette Stove. *Renewable and Sustainable Energy Reviews*, 1–6. <http://dx.doi.org/10.23919%2FICUE.2017.8068008>
- [80] Trubetskaya, A., Leahy, J. J., Yazhenskikh, E., Müller, M., Layden, P., Johnson, R., Ståhl, K., & Monaghan, R. F. D. (2019). Characterization of woodstove briquettes from torrefied biomass and coal. *Energy*, 171, 853–865. <https://doi.org/10.1016/j.energy.2019.01.064>
- [81] Verma, P., & Shukla, S. K. (2019). Performance evaluation of improved cook stove using briquette as fuel. *AIP Conference Proceedings*, 1–12. <https://doi.org/https://doi.org/10.1063/1.5096492>
- [82] Wang, D., Liu, L., Yuan, Y., Yang, H., Zhou, Y., & Duan, R. (2019). Design and key heating power parameters of a newly-developed household biomass briquette heating boiler. *Renewable Energy*, 1–19. <https://doi.org/10.1016/j.renene.2019.09.081>
- [83] Yang, I., Cooke-willis, M., Song, B., & Hall, P. (2021). Densification of torrefied Pinus radiata sawdust as a solid biofuel: Effect of key variables on the durability and hydrophobicity of briquettes. *Fuel Processing Technology*, 214, 1–9. <https://doi.org/10.1016/j.fuproc.2020.106719>
- [84] Yang, Y., Chu, M., Hao, C., & Zhou, L. (2019). Preparation of low silicon ultra clean coal by flotation pretreatment followed by alkali-acid leaching combined process. *Energy Sources, Part A: Recovery, Utilization, and Environmental Effects*, 1–16. <https://doi.org/10.1080/15567036.2019.1665149>
- [85] Zhang, L., Li, Z., Yang, Y., Zhou, Y., Kong, B., Li, J., & Si, L. (2016). Effect of acid treatment on the characteristics and structures of high-sulfur bituminous coal. *Fuel*, 184, 418–429. <https://doi.org/10.1016/j.fuel.2016.07.002>
- [86] Zhao, H., Bai, Z., Bai, J., Guo, Z., Kong, L., & Li, W. (2015). Effect of coal particle size on distribution and thermal behavior of pyrite during pyrolysis. *Fuel*, 148, 145–151. <https://doi.org/10.1016/j.fuel.2015.01.104>
- [87] Zhong, Q., Yang, Y., Li, Q., Xu, B., & Jiang, T. (2017). Coal tar pitch and molasses blended binder for production of formed coal briquettes from high volatile coal. *Fuel Processing Technology*, 157, 12–19. <https://doi.org/10.1016/j.fuproc.2016.11.005>